Journal of Electroceramics 2:1, 49–55, 1998

Electrical Conduction and Disorder in the Pyrochlore System $(Gd_{1-x}Ca_x)_2Sn_2O_7$

T.-H. YU & H.L. TULLER

Crystal Physics and Electroceramics Laboratory, Department of Materials Science and Engineering, Massachusetts Institute of Technology, Cambridge, MA 02139, USA

Received July 7, 1997; Accepted December 18, 1997

Abstract. Electrical conductivity measurements were made on the pyrochlore compounds $(Gd_{1-x}Ca_x)_2Sn_2O_7$ ($x = 0$, 0.0036, 0.0057, 0.03) as a function of temperature, oxygen partial pressure and Ca doping concentration. An effective Frenkel constant and oxygen vacancy mobility were derived. Intrinsic anion disorder was found to be lower than the expected value based on the relative radii of the cations in the A and B sites ($A_2B_2O_7$). Low oxygen vacancy mobilities as well as low anion disorder resulted in considerably lower ionic conductivities in $Gd_sSn_2O_7$ relative to the previously studied $Gd_2(Ti_{1-x}Zr_x)_2O_7$ system. The temperature and composition dependence of the *p*-type electronic conductivity were evaluated and the oxidation enthalpy was derived.

Keywords: stannate pyrochlore, anion disorder, oxygen vacancy mobilities, ionic conductivity

Introduction

Oxides with the pyrochlore structure exhibit a wide range of ionic and electronic conductivities depending on composition. The rare earth pyrochlore $Gd_2(Ti_{1-x}Zr_x)_2O_7$ (GZT) has been investigated as a potential solid oxide electrolyte in solid oxide fuel cells and related systems [1]. At lower Zr fraction, substantial mixed ionic-electronic conduction (MIEC) was found to exist. Above Zr fractions of 0.3, the oxygen ion conductivity was found to increase sharply with increasing x. This increase in ionic conductivity was related to an increase in anion disorder with increasing Zr content as confirmed by neutron diffraction experiments on the closely related $Y_2(Ti_{1-x}Zr_x)_2O_7$ (YZT) system [2]. From these studies, it was concluded that one of the key parameters influencing structural disorder in $A_2B_2O_7$ pyrochlores was the cation radius ratio, namely r_A/r_B. As r_B approaches r_A, disorder in both the cation and anion sublattices increases ultimately reaching complete disorder characteristic of the fluorite structure as in the case of $Y_2Zr_2O_7$ (YZ) [2]. As the larger Zr ion replaces Ti on the B site of GZT and YZT, increasing anion disorder results in orders of magnitude increases in the oxygen ion conductivity.

Following the ionic radii charts of Shannon and Prewitt [3] in six-fold coordination, one obtains an ionic radius of Sn^{4+} of 0.69 Å which lies between that of Ti^{4+} (0.605 Å) and Zr^{4+} (0.72 Å). The question arises if the degree of disorder in $Gd_2Sn_2O_7$ (GS) would be comparable to that in GZT with the same average B cation radius. The purpose of this research is to investigate whether Sn^{4+} would also contribute to disorder in related pyrochlores thereby confirming that the disorder in pyrochlores is truly a function of r_A/r_B regardless of the chemistry of the B site cation.

For the titanium end member, $Gd_2Ti_2O_7$ (GT), where intrinsic disorder is minimal due to the small ionic radius of Ti^{4+}, the ionic conductivity is dramatically increased by the addition of the aliovalent dopant Ca^{2+} on the A site. A maximum ionic conductivity of 5×10^{-2} S/cm is reached at 1000°C with GT + 8 mol% Ca [4]. In this investigation, we chose to investigate the system $(Gd_{1-x}Ca_x)_sSn_2O_7$. By examining the relative influence of Ca mole fraction on the ionic conductivity, one may, with the assistance of the appropriate

defect model, extract the value of the intrinsic disorder as previously done in the system $(Gd_{1-x}Ca_x)_2(Zr_{0.3}Ti_{0.7})_2O_7$ [5].

Theory

The pyrochlore structure has a number of empty interstitial sites which would be viewed as oxygen vacancies in the defect fluorite structure. There are two crystallographic sites (48f, 8a) for oxygen ions in ordered pyrochlores. Oxygen ions located at 48f sites can be exchanged with empty interstitial 8b sites at high temperature as observed from neutron diffraction studies [2]. This exchange creates anion Frenkel defects consisting of an oxygen interstitial–vacancy pair as described below:

$$O_0 \leftrightarrow O_i'' + V_0^{\bullet\bullet}$$
$$K_F = [V_0^{\bullet\bullet}][O_i''] = K_{FO}\exp(-E_F/\mathrm{kT}) \quad (1)$$

where E_F represents the Frenkel formation energy and the remaining terms follow standard Kröger–Vink defect notation.

The oxidation reaction which describes the annihilation of oxygen vacancies and the creation of holes by absorption of oxygen from the gas phase is given by:

$$V_0^{\bullet\bullet} + 1/2O_2 \leftrightarrow O_0 + 2h^{\bullet}$$
$$K_{ox} = p^2[V_0^{\bullet\bullet}]^{-1}\mathrm{Po_2}^{-1/2} = K_{oxo}\exp(-E_{ox}/\mathrm{kT}) \quad (2)$$

where E_{ox} represents the oxidation energy.

Intrinsic electron–hole pair generation is given by:

$$\mathrm{nil} \leftrightarrow e' + h^{\bullet}$$
$$K_e = np = K_{eo}\exp\left(-E_g/\mathrm{kT}\right) \quad (3)$$

where E_g represents the thermal band gap.

Electroneutrality requires a balance of charged species. This is represented by:

$$2[V_0^{\bullet\bullet}] + p + [D^{\bullet}] = [A'] + n + 2[O_i''] \quad (4)$$

in which A' and $D^{\bullet}$ represent singly ionized acceptors and donors. For materials which are predominantly ionic conductors, $n, p \ll [V_0^{\bullet\bullet}], [O_i'']$ [6].

Combining Eqs. (1)–(4) and solving for $[V_0^{\bullet\bullet}]$ after assuming negligible n and p yields:

$$[V_0^{\bullet\bullet}] = 0.25[I + (I^2 + 16K_F)^{1/2}] = R \quad (5)$$

$$n = K_e(K_{ox}R)^{-1/2}\mathrm{Po_2}^{-1/4} \quad (6)$$

$$p = (K_{ox}R)^{1/2}\mathrm{Po_2}^{1/4} \quad (7)$$

where $I = [A'] - [D^{\bullet}]$ is the net acceptor concentration. Oxygen interstitials have been shown previously [5] to contribute to a negligible degree to the ionic conductivity and so are not treated further.

The ionic conductivity can be obtained by multiplying Eq. (5) by its effective charge (2e) and mobility (μ_i).

$$\sigma_i = 0.5[I + (I^2 + 16K_F)^{1/2}]e\mu_i \quad (8)$$

Eq. (8) shows that one can obtain the Frenkel constant and oxygen vacancy mobility from a measurement of the ionic conductivity as a function of dopant concentration by fitting the experimental data to Eq. (8) using the iterative least square minimization routine. The ionic conductivity may also be written in the more general form:

$$\sigma_i = \frac{\sigma_0}{T}\exp(-E_i/\mathrm{kT}) \quad (9)$$

in which E_i contains terms related to defect formation (e.g., E_F) and migration terms E_m.

Multiplying each of the mobile charge carriers ($V_0^{\bullet\bullet}$, e', $h^{\bullet}$) by their mobilities and summing the three terms gives an expression for the total conductivity.

$$\sigma_{tot} = \sigma_i + \sigma_e + \sigma_h = A + B(\mathrm{Po_2})^{-1/4} + C(\mathrm{Po_2})^{1/4} \quad (10)$$

Note that while the concentrations of n and p relative to $V_0^{\bullet\bullet}$and O_i'' may be small, because of their much higher mobilities, they may still contribute significantly to σ_{tot} [6].

Since each contribution to the total conductivity in Eq. (10) is distinguished by a unique Po_2 dependence, this allows one to readily isolate the ionic conductivity by analyzing the Po_2-dependence of the conductivity.

Experimental Procedures

Powders were prepared by a liquid-mix technique [7] with compositions $(Gd_{1-x}Ca_x)_2Sn_2O_7$ ($x = 0$, 0.0036, 0.0057, 0.03). This process allows one to produce ceramic powder with well-defined cation mole ratios and near atomic scale mixing. Based on earlier studies of Ca doped GT [4], Ca substitution for Gd in GS is expected, with the resultant formation of singly

ionized acceptors (Ca_{Gd}'). After calcination at 850°C, the powders were die pressed at 4 Kpsi, isopressed at 40 Kpsi and then sintered at 1550°C for 16 h. X-ray diffraction data confirmed the formation of the pyrochlore phase with superlattice peaks which distinguish the pyrochlore from the defect fluorite phase. Microprobe analysis was used to measure the Ca doping levels. The analyzed levels tended to be below the intended values.

Electrical conductivity measurements were performed on sintered bar-shaped samples with four probe configuration. Two and four probe dc conductivity measurements were performed with an HP4140b picoammeter and Keithley 188 nanovoltmeter. Impedance spectroscopy measurements were performed with an HP4192A impedance analyzer to separate bulk, grain boundary and electrode conductivities. The temperature range examined was from 800–1050°C in 50° increments and the Po_2 ranged from $10^{-15} - 1$ atm. Exposure to more reducing atmospheres resulted in decomposition and the appearance of a monoclinic phase, Gd_2SnO_5 as evidenced by X-ray diffraction.

Results

Figure 1 gives the Po_2-dependence of the total conductivity of GS for a number of isotherms. The data were fitted to Eq. (10) by least square analysis to extract the parameters A, B and C which were used to produce the solid curves shown in the Fig. 1. *P*-type conduction with a $Po_2^{1/4}$ dependence at high Po_2 is observed followed by a Po_2-independent plateau at intermediate and low Po_2 attributed to ionic conduction. The ionic conduction, for example, is observed down to a Po_2 of 10^{-15} atm at 800°C. Exposure to more reducing atmospheres resulted in decomposition of the phase as evidenced by X-ray diffraction and a sharp decrease in conductivity. Compared with GZT with high Zr content ($x \geqslant 0.4$) [1], undoped GS has an ionic conductivity lower by two orders of magnitude than that of GZT. This unexpected result appears to run counter to the assumption that disorder increases with increasing average B site cation radius as the ionic radius of Sn is comparable to that of Zr. Significant *p*-type conduction at high Po_2 is also a distinctive difference as compared with GZT which exhibited weak or no *p*-type conduction at high Po_2.

Figures 2 to 4 show the total conductivity of $(Gd_{1-x}Ca_x)_2Sn_2O_7$ for various Ca dopant levels ($x = 0.0036$, 0.0057 and 0.03). These show that GS doped with Ca exhibits a similar dependence of total conductivity on Po_2 as does undoped GS. The ionic component of the total conductivity, extracted from the log σ versus log Po_2 data with the aid of Eq. (10) for all four compositions is shown plotted in Fig. 5 versus reciprocal temperature. The ionic conductivities

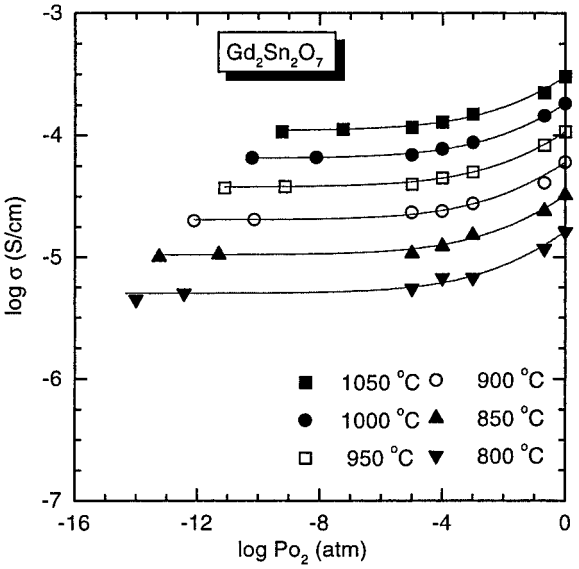

Fig. 1. Log conductivity versus log oxygen partial pressure for $Gd_2Sn_2O_7$.

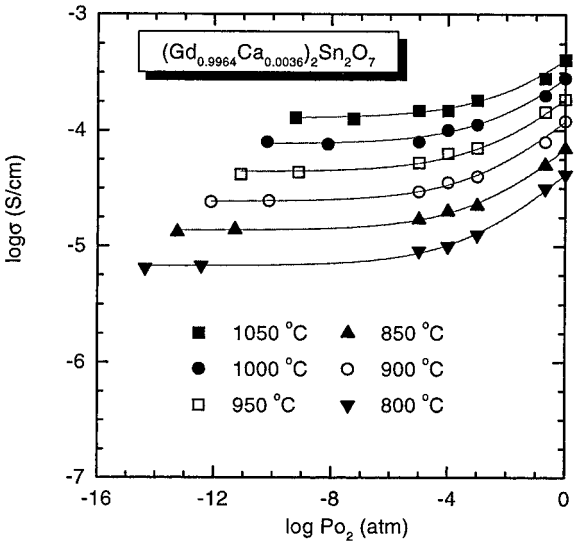

Fig. 2. Log conductivity versus log oxygen partial pressure for $(Gd_{1-x}Ca_x)_2Sn_2O_7$ with $x = 0.0036$.

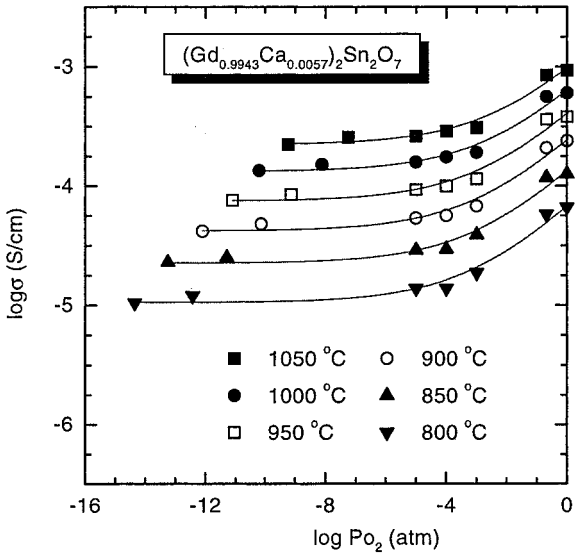

Fig. 3. Log conductivity versus log oxygen partial pressure for $(Gd_{1-x}Ca_x)_2Sn_2O_7$ with $x = 0.0057$.

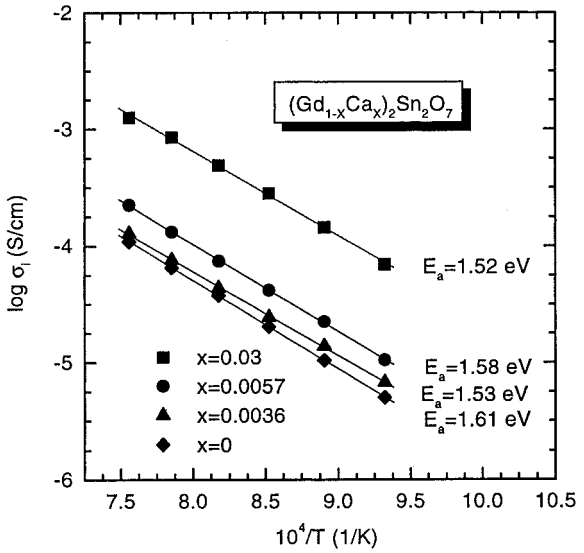

Fig. 5. The temperature dependence of the ionic conductivity for $(Gd_{1-x}Ca_x)_2Sn_2O_7$.

derived for GS ($x = 0.0036$) are in excellent agreement with recently reported oxygen self diffusion measurements [8]. Note that while the specimens with $x = 0.0036$ and $x = 0.0057$ show only small increases in ionic conductivity over undoped GS, the specimen with $x = 0.03$ exhibits an ionic conductivity approximately 12 times greater in magnitude.

The activation energy, E_i, and pre-exponential constant, σ_o for the bulk ionic conductivity were calculated for these compositions (see Eq. (9)) and are shown plotted in Fig. 6. The derived activation energies, which range from $1.52 \sim 1.61$ eV, are approximately double those found for ionic conduction in GZT. The pre-exponential constant increases with increasing Ca content above $x = 0.0036$ reaching $\sim 10^6$ S/cmK at GS with 3% Ca while the

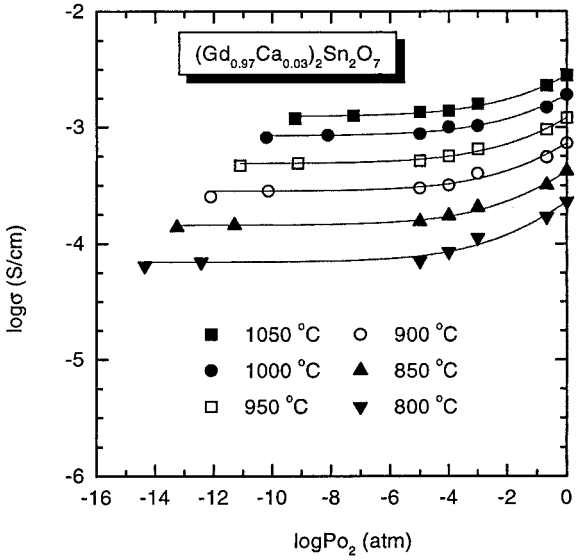

Fig. 4. Log conductivity versus log oxygen partial pressure for $(Gd_{1-x}Ca_x)_2Sn_2O_7$ with $x = 0.03$.

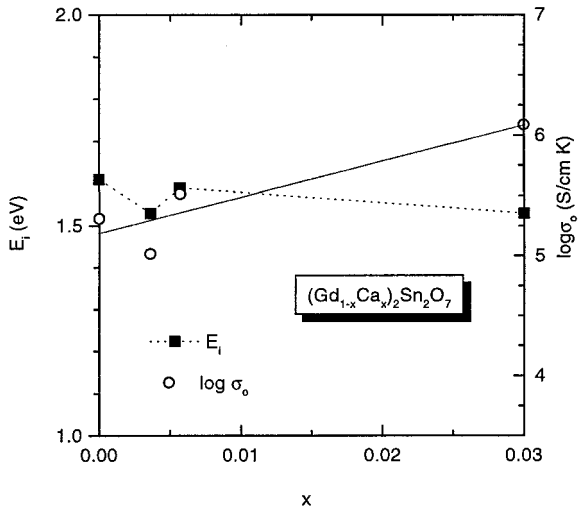

Fig. 6. The activation energy and the pre-exponential constant for ionic conduction as a function of x for $(Gd_{1-x}Ca_x)_2Sn_2O_7$.

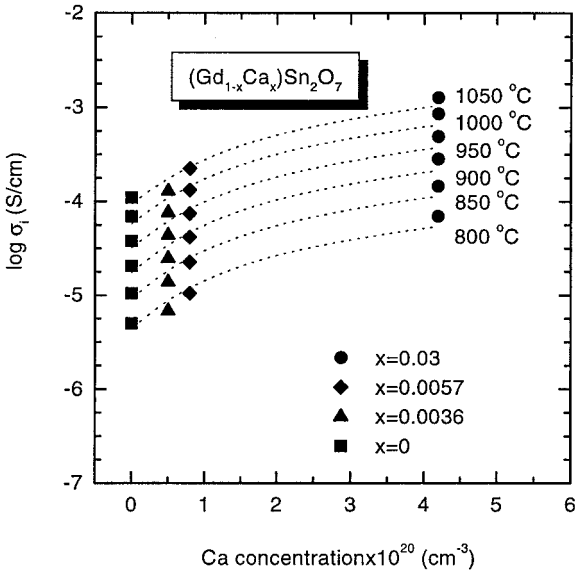

Fig. 7. The ionic conductivity as a function of Ca concentration for $(Gd_{1-x}Ca_x)_2Sn_2O_7$.

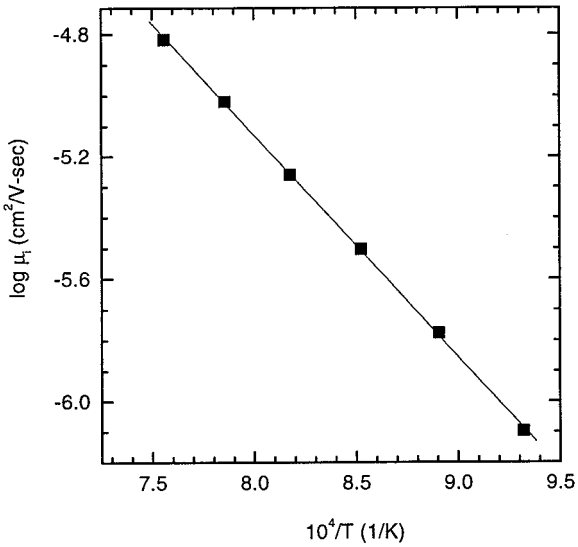

Fig. 9. Calculated values for the oxygen vacancy mobility in $Gd_2Sn_2O_7$ as a function of 1/T.

activation energy remains relatively insensitive to the Ca concentration.

The isothermal composition dependence of the ionic conductivity of GS on Ca content is shown plotted in Fig. 7. These data were fit to Eq. (8) in an attempt to extract values for K_F and μ_i. Figures 8 and 9 represent the derived values of K_F and μ_i at each of the isotherms and the fits through these data result in the following expressions.

$$K_F = 1.165 \times 10^{39} \times \exp(-0.13 \pm 0.06 \text{ eV/kT}) \text{ cm}^{-6}$$

$$\mu_i = \frac{1.518 \times 10^4}{T} \times \exp(-1.54 \pm 0.03 \text{ eV/kT}) \text{ cm}^2/\text{V}$$

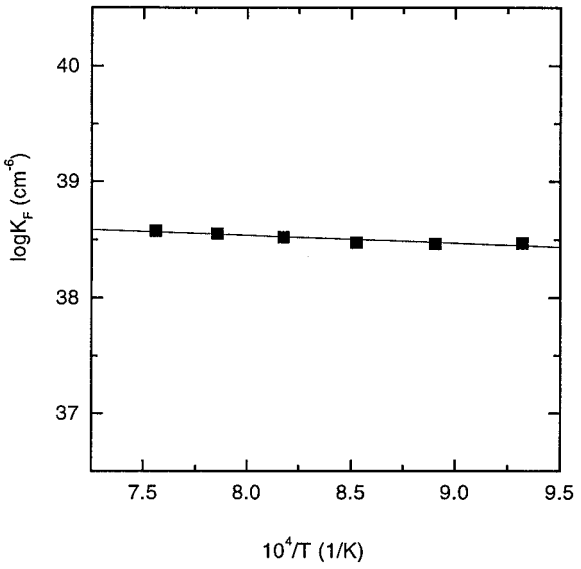

Fig. 8. Calculated values for the Frenkel constant in $Gd_2Sn_2O_7$ as a function of 1/T.

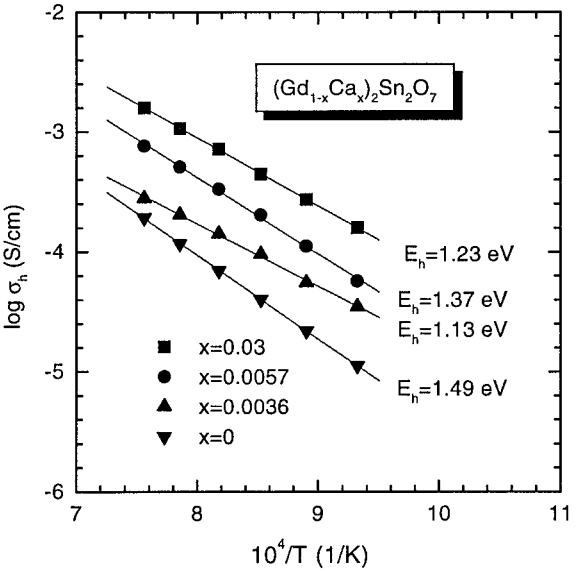

Fig. 10. The temperature dependence of *p*-type conductivity for $(Gd_{1-x}Ca_x)_2Sn_2O_7$ at Po_2 of 1 atm.

The *p*-type conductivity is shown plotted versus reciprocal temperature in Fig. 10 at $Po_2 = 1$ atm for pure GS and Ca doped GS. While the activation energies for *p*-type conduction, E_h, range from 1.13–1.49 eV, they typically fall within the range of 1.35 ± 0.15 eV. The *p*-type conductivity was also found to increase nearly linearly with Ca content between 0.36 and 3%.

Discussion

The magnitude of the Po_2 independent-ionic conductivity in undoped GS ($\sim 10^{-4}$ S/cm at 1000°C) was found to be several orders of magnitude lower than that in GZT with Zr content ($x = 0.8$) having a comparable r_A/r_B ratio. The question arises as to the source of the low ionic conductivity in GS. The ionic conductivity consists of two parts—carrier concentration and mobility. We first examine the carrier concentration, which is the oxygen vacancy concentration in the case of acceptor doped or intrinsically disordered pyrochlores [1]. As mentioned above, the r_A/r_B ratio was found to be an important factor in determining intrinsic disorder in GZT. From a lattice constant comparison, $Gd_2(Ti_{0.2}Zr_{0.8})_2O_7$ has the same average B site cation radius as GS. It has been estimated from the pre-exponential term, σ_o, that the oxygen vacancy density is $\sim 0.85\%$ in $Gd_2(Ti_{0.2}Zr_{0.8})_2O_7$ [1].

Figure 5 shows that the ionic conductivity of GS is increased by order of magnitude with 3% Ca^{2+} doping. In the case of Ca doped GT [4], 2% Ca doping on the A site of GT increased the ionic conductivity by orders of magnitude by introducing extrinsically generated oxygen vacancies into the highly ordered anion lattice. This difference indicates that the anion lattice in GS has a higher number of oxygen vacancies compared with those in GT. Figure 6 shows that E_i remains relatively insensitive to Ca doping in GS. Thus as shown in the figure, the increases in ionic conductivity with Ca-doping is, therefore, related to increases in σ_o. Using the values of $3.562 \times 10^{38}\,cm^{-6}$ obtained for the Frenkel constant at 1000°C and Eq. (1), an oxygen vacancy density of 0.045% is obtained. This is much lower than that of 0.85% estimated for $Gd_2(Ti_{0.2}Zr_{0.8})_2O_7$. From the ionic conductivity data in GZT, we can estimate the GZT composition which has comparable anion disorder to that of GS. In GZT, an order of magnitude increase in ionic conductivity was observed as x increases from 0.3 to 0.8 [1]. Since the oxygen vacancy mobility remains the same in GZT, this increase in the ionic conductivity is attributed to the increase in oxygen vacancy concentration. The Frenkel constant for GS is much closer to that obtained for GZT ($x = 0.3$) of $1.0 \times 10^{39}\exp(-0.24$ eV/kT) [5], lower than the expected value based on the ionic radius ratio. The magnitude of the pre-exponent of the Frenkel constant, K_{FO}, of $1.165 \times 10^{39}\,cm^{-6}$ was found to be lower than the product of oxygen lattice and interstitial sites (48f and 8b sites) of $2.932 \times 10^{44}\,cm^{-6}$ expected in the ideal case, where the concentration of defects is sufficiently small to neglect the defect interactions under constant volume conditions [9]. This suggests significant interaction between defect species in GS.

Table 1 shows the effective Frenkel formation energy derived experimentally for a number of related pyrochlores as a function of the r_A/r_B ratio. The Frenkel defect energy of 0.13 eV calculated from the GS data follows the decreasing trend in E_F with decreasing r_A/r_B in $A_2B_2O_7$ pyrochlores, i.e., 0.44 eV in GZT ($x = 0.25$) [4] and 0.24 eV in GZT ($x = 0.3$) [5]. This trend is consistent with expectations that the pyrochlores more easily disorder as r_B approaches r_A in magnitude.

The oxygen vacancy mobility is also found to be lower than that of GZT. At 1000°C, GS is calculated to have an oxygen vacancy mobility of $8.6 \times 10^{-6}\,cm^2/V \cdot s$. This is remarkably low for pyrochlore oxides. The calculated value for oxygen vacancy mobility in GZT at $x = 0.3$ at 1000°C is $1.2 \times 10^{-4}\,cm^2/V \cdot s$ with an activation energy of 0.78 eV [5], less than half of that in GS of 1.54 eV. This high value of the oxygen vacancy migration energy is rather unexpected considering that pyrochlores are more ordered relative to fluorites, leading to improved oxygen vacancy mobility. High values of E_i were also observed in the solid solutions of $Gd_2(Zr_{1-x}Sn_x)_2O_7$ and $Gd_2(Ti_{1-x})_2O_7$ [10]. In both

Table 1. The Frenkel energy as a function of r_A/r_B in $A_2B_2O_7$ pyrochlores. The data for GZT $x = 0.25$ and $x = 0.3$ are from [4] and [5] respectively

Composition	r_A/r_B	E_F (eV)
$Gd_2(Ti_{0.75}Zr_{0.25})_2O_7$	1.674	0.44
$Gd_2(Ti_{0.7}Zr_{0.3})_2O_7$	1.658	0.24
$Gd_2Sn_2O_7$	1.536	0.13

systems, E_i increases with increasing Sn content resulting in a decrease in oxygen vacancy mobility.

The low conductivity in GS indicates the importance of local bonding on anion disorder and mobility. Vandenborre et al. [11] suggested that the Sn-O bonding is more rigid and covalent compared with that between Ti-O as reflected in the strong force field in Sn-O bonding. From the refinement of Raman spectra in pyrochlores, the stretching constant between the B cation and oxygen ion was found to be 1.27×10^2 Nm^{-1} for $Gd_2Ti_2O_7$ and 1.73×10^2 Nm^{-1} for $Gd_2Sn_2O_7$. The authors attributed a part of the increase to the higher electronegativity of Sn^{4+} in comparison with the Ti^{4+} and Zr^{4+} cations. From the electronic structure calculations by Svane and Antoncik [12], an appreciable degree of covalency in the bonding was observed for SnO_2 in contrast to the significant ionic character in TiO_2. Since oxygen ions are surrounded by four cations and have to overcome the potential barriers induced by the cations to migrate through the lattice, it is expected that the bonding characteristics between cation and anion can impact the mobility significantly.

We next examine the p-type conductivity. By review of Eq. (7), we observe that $p \propto (K_{ox}R)^{1/2}$. Even in the limit where $R = K_F{}^{1/2}$, this adds a negligible contribution to the temperature dependence i.e., $E_{F/4} \cong 0.026$ eV. Consequently the activation energy derived from Fig. 10, $E_h \cong 1.35 \pm 0.15$ eV should correspond largely to $E_{ox} + E_H$ where E_H is the hole hopping energy in the case of small polaron transport. In related studies in GZT [13], E_H for holes was estimated to be nearly zero. Therefore $E_{ox} \cong 2E_h \approx 2.70 \pm 0.30$ eV. This value is somewhat larger than values of E_{ox} obtained earlier for $Gd_2(Zr_{0.3}Ti_{0.7})_2O_7$ of 2.2 ± 0.4 eV [14].

Summary

Electrical conductivity measurements were performed on the pyrochlore compound $Gd_2Sn_2O_7$ doped with Ca at levels of 0, 0.0036, 0.0057, and 0.03. The effective Frenkel constant derived from application of our defect model indicates a substantial intrinsic disorder of $\sim 0.05\%$, but lower than that in $Gd_2(Ti_{0.2}Zr_{0.8})_2O_7$ with comparable r_A/r_B ratio. Oxygen vacancy mobilities in $Gd_2Sn_2O_7$ were also found to be low compared with $Gd_2(Ti_{1-x}Zr_x)_2O_7$ system, with a correspondingly low oxygen ion conductivity of $\sim 10^{-4}$ S/cm at 1000°C. The low oxygen vacancy mobilities and low anion disorder in $Gd_2Sn_2O_7$ points to the importance of the more covalent nature of the Sn-O as compared to the Ti-O and Zr-O bonds. The temperature and composition dependence of the p-type electronic conductivity were evaluated and the oxidation enthalpy derived.

Acknowledgment

This work was supported by the Department of Energy, Division of Materials Science, Office of Basic Energy Research under grant #DE-FG02-86ER45261.

References

1. P.K. Moon and H.L. Tuller, in *Solid State Ionics*, edited by G. Nazri, R.A. Huggins, and D.F. Shriver (Mater. Res. Soc. Symp. Proc. **135**, Pittsburgh, PA, 1989), p. 149.
2. C. Heremans, B.J. Wuensch, J.K. Stalick, and E. Prince, in *Solid State Ionics III*, edited by G. Nazri, J. Tarascon and M. Armand (Mater. Res. Soc. Symp. Proc. **293**, Pittsburgh, PA, 1993), p. 349.
3. R.D. Shannon and C.T. Prewitt, *Acta Cryst*., **B25**, 925 (1969).
4. S. Kramer, Mixed Ionic-Electronic Conduction in Rare Earth Titanate/Zirconate Pyrochlore Compounds, Ph.D. Thesis, Massachusetts Institute of Technology, Cambridge (1994).
5. P.K. Moon and H.L. Tuller, *Solid State Ionics*, **28–30**, 470 (1988).
6. H.L. Tuller, in *Nonstoichiometric Oxides*, edited by O.T. Sorensen (Academic Press, NY, 1981), p. 275.
7. M.P. Pechini, US Patent No. 3,330,697 (1967).
8. A.C.S. Sabioni, T.-H. Yu, and H.L. Tuller, to be published in Proc. 3rd Int. Symp. on Ionic and Mixed Conducting Ceramics, 192 meeting of the Electrochem. Soc., Paris, 9/3-8/97.
9. N.N. Greenwood, in *Ionic Crystals, Lattice Defects and Nonstoichiometry* (Butterworth & Co., London, 1968).
10. Tae-Hwan Yu and H.L. Tuller, *Solid State Ionics*, **86–88**, 177 (1996).
11. M.T. Vandenborre, E. Husson, J.P. Chartry, and D. Michel, *J. Raman Spectroscopy*, **14**, 63 (1983).
12. A. Svane and E. Antoncik, *J. Phys. Chem. Solids*, **48**, 171 (1987).
13. M.A. Spears and H.L. Tuller, in *Solid State Ionics III*, edited by G. Nazri, J. Tarascon and M. Armand (Mater. Res. Soc. Symp. Proc. **293**, Pittsburgh, PA, 1993), p. 301.
14. P.K. Moon, Electrical Conductivity and Structural Disorder in $Gd_2Ti_2O_7$–$Gd_2Zr_2O_7$ Solid Solutions, Ph.D. Thesis, Massachusetts Institute of Technology, Cambridge (1988).